Thermodynamics of hydrogen adsorption on calcium exchanged faujasite-type zeolites

G.T. Palomino[a], B. Bonelli[b], C.O. Areán[a], J.B. Parra[c], M.R.L. Carayol[a], M. Armandi[b], C.O. Ania[c], E. Garrone[b,*]

[a] Departamento de Química, Universidad de las Islas Baleares, 07122 Palma de Mallorca, Spain
[b] Dipartimento di Scienza dei Materiali ed Ingegneria Chimica, Politecnico di Torino, 10129 Turin, Italy, and INSTM Unit of Torino Politecnico.
[c] CSIC, Instituto Nacional del Carbón, Apdo. 73, E-33080 Oviedo, Spain

Abstract
A combination of variable-temperature infrared spectroscopy with volumetric gas adsorption measurements was used to study the thermodynamics of hydrogen adsorption, at a low temperature, on calcium-exchanged zeolites X and Y. Two adsorption regimes were considered: (i) localized adsorption of dihydrogen molecules on Ca^{2+} cation sites, and (ii) delocalized hydrogen adsorption following saturation of the Ca^{2+} adsorbing centres. For localized adsorption, the corresponding enthalpy change was found to be in the range of -12 to -15 kJ mol^{-1}, while the isosteric heat of delocalized adsorption was found to be in the range of -5 to -6 kJ mol^{-1}. These experimental results are discussed in the broader context of corresponding data for other alkaline zeolites, with a focus on correlation between adsorption enthalpy and entropy for the localized adsorption regime.

1. Introduction

The search for materials capable of safe and cost effective storage and on-board transport of hydrogen constitutes a major issue in the energy sector; among solutions being sought, porous adsorbents constitute a main line of current research [1,2]. These materials comprise mainly active carbons, including carbon nanostructures [3-8], and porous metal-organic frameworks (MOFs) and related materials [9-15]. Because of the high density of the aluminosilicate framework, which results in a low gravimetric uptake of the adsorbed gas, zeolites themselves are not likely candidates for on-board hydrogen storage and delivery. However, well known crystal structure and easy ion exchange make zeolites ideal materials for systematic studies on hydrogen bonding to a wide variety of metal-cation centres. And the realization that such studies can lead to useful insights for designing more prospective hydrogen adsorbents (*e.g.* MOFs having

exposed cation sites) lead to examine in detail hydrogen adsorption on zeolites, focusing attention on the gas-solid interaction energy; both experimental [16-21] and theoretical [22-26] studies were recently reported by several research groups.

We report here on experimental studies on hydrogen adsorption on calcium-exchanged faujasites, types X and Y. Gas adsorption isotherms (at 77.3 and 90.2 K) were used to derive the corresponding isosteric heat of adsorption and its variation with surface coverage, while variable temperature infrared spectroscopy was used to determine hydrogen adsorption enthalpy and entropy, thus achieving a fairly complete thermodynamic characterization of the gas adsorption process. The results are discussed in the broader context of available data for hydrogen adsorption on other alkali and alkaline-earth cation exchanged zeolites, with a view to gain further knowledge on the influence of exposed (coordinatively unsaturated) metal cations on hydrogen adsorption on porous solids, and also to highlight the important role played by the adsorption entropy.

2. Materials and methods

Faujasite-type zeolites X and Y were synthesized in their sodium forms by following standard procedures [27]; they had Si:Al ratios of 1.5 and 2.7, respectively. These parent materials were then repeatedly exchanged with a 0.5 M solution of calcium nitrate. Chemical analysis showed that practically total exchange of calcium for sodium was attained (only traces of sodium were found) in the case of the X zeolite, while for the Y zeolite only a partial exchange was attained. Hence, the calcium-exchanged samples are hereafter termed Ca-X and (Ca,Na)-Y, respectively. Powder X-ray diffraction of these samples showed good crystallinity in both cases, and all diffraction lines could be assigned to the corresponding faujasite-type structure [28].

Low temperature (77.3 and 90.2 K) hydrogen adsorption isotherms on Ca-X and (Ca,Na)-Y samples were measured on a Micromeritics ASAP 2010M gas adsorption analyser, up to atmospheric pressure. For these hydrogen adsorption measurements, the zeolite samples were previously outgassed under a dynamic vacuum (*ca*. 10^{-2} Torr, 1 Torr = 1.32 mbar) at 673 K overnight; subsequently, they were further outgassed for a short time at the same temperature under an ultra-high vacuum (*ca*. 10^{-6} Torr). Each adsorption isotherm was measured along 24 h, allowing for over one hundred equilibrium points to be registered. High purity hydrogen (premier quality) was supplied

by Metal Carbides. From the adsorption isotherms thus recorded, corresponding values of isosteric heat of adsorption were obtained by using the corresponding computer program supplied by Micromeritics.

For infrared (IR) spectroscopy, a thin self-supported wafer of each sample was prepared and activated (outgassed) in a dynamic vacuum (residual pressure < 10^{-4} Torr) for 3 h at 673 K inside a home made IR cell, described elsewhere [29], which allowed in situ sample activation, gas dosage and variable temperature IR spectroscopy to be carried out. After recording the blank spectrum of the zeolite wafer at liquid nitrogen temperature the cell was dosed with hydrogen, it was then closed, and spectra were taken at several fixed temperatures (within the range of 78 to 140 K) while simultaneously registering temperature and hydrogen equilibrium pressure inside the cell. For that purpose, the IR cell was equipped with a platinum resistance thermometer (Tinsley) and a capacity pressure gauge (Baratron). The precision of these measurements was about ±2 K and $\pm 2\times10^{-2}$ Torr, respectively. Fourier transform IR spectra were recorded, at 3 cm^{-1} resolution, by using a Bruker IFS66 instrument; 64 scans were accumulated for each spectrum.

It should be noted that localized adsorption of hydrogen molecules on zeolite alkali and alkaline-earth (extra-framework) cations leads to activation in the IR of the H–H stretching mode, which shows the characteristic IR absorption band red-shifted from the wavenumber value of the corresponding (Raman-active) mode of gas-phase molecular hydrogen [30-32]. This characteristic IR absorption band of adsorbed hydrogen, which usually appears in the range of 4050-4110 cm^{-1}, can be used to monitor adsorption thermodynamics by following the variable temperature IR (VTIR) spectroscopic method which in its very essence is outlined below in order to facilitate understanding of this article. Further details of the method can be found elsewhere [33,34].

At any given temperature, the integrated intensity of the characteristic IR absorption band (of adsorbed hydrogen) should be proportional to surface coverage, θ, thus giving information on the activity of both the adsorbed species and the empty adsorbing sites; simultaneously, the equilibrium pressure gives the activity of the gas-phase. Hence, the corresponding adsorption equilibrium constant, K, can be determined, and the variation of K with temperature leads to the corresponding values of standard adsorption enthalpy (ΔH^{o}) and entropy (ΔS^{o}). For deriving these values, integrated band

intensity, A, temperature, T, and equilibrium pressure, p, are considered to be interrelated by the Langmuir-type equation:

$$\theta = A/A_M = K(T)\, p / [1 + K(T)\, p] \quad (1)$$

where A_M stands for the integrated band intensity corresponding to full coverage ($\theta = 1$). Combination of Eq. (1) with the well known van't Hoff equation (2) leads to Eq. (3) below:

$$K(T) = \exp(-\Delta H^0/RT)\exp(\Delta S^0/R) \quad (2)$$

$$\ln[A/(A_M - A)p] = (-\Delta H^0/RT) + (\Delta S^0/R) \quad (3)$$

By plotting the left-hand side of Eq. (3) against reciprocal temperature, for data obtained over a relatively large temperature range, corresponding values of ΔH^0 and ΔS^0, assumed to be temperature-independent, can directly be derived.

3. Results and discussion

Fig. 1 shows variable-temperature FTIR spectra, in the H–H stretching region, of hydrogen adsorbed on the zeolite Ca-X. A single H–H stretching band is seen, centred at 4082 cm^{-1}. This IR absorption band corresponds to the dihydrogen molecule polarized by Ca^{2+} ions. Polarization, which is known to be the driving force for H_2 adsorption [21,23,24], renders IR-active the fundamental H–H stretching mode, which is only Raman-active (at 4163 cm^{-1}) for the free dihydrogen molecule. Such a polarization also brings about a bathochromic shift of ν(H–H) which, in general terms, is proportional to the polarizing power of the cation involved [18,21,35]. However, the detailed structure of the cationic adsorbing centre (which includes the cation and nearby anions of the zeolite framework) is also known to have an influence on the magnitude of the bathochromic shift [21,30, 31]. Hence, the actual value of ν(H–H) depends on both, the extra-framework cation involved and the zeolite being considered. Corresponding variable-temperature FTIR spectra of hydrogen adsorbed on the zeolite (Ca,Na)-Y are shown in Fig. 2. The IR absorption band of H_2 interacting with Ca^{2+} ions is now seen at

4078 cm^{-1}. An additional (much weaker) band was also seen at 4125 cm^{-1} (not shown) and assigned, in agreement with literature reports [31,36], to hydrogen interacting with Na^+ ions. This latter band, which comes from an incomplete ion exchange of Ca^{2+} for Na^+ in the parent Na-Y zeolite, is of no concern here.

From the sets of variable-temperature IR spectra shown in Figs. 1 and 2, the linear plots of Eq. (3) shown in Fig. 3(a,b) were obtained. From these linear plots, the standard adsorption enthalpy was found to be ΔH^0 = -12.5 kJ mol^{-1} for hydrogen on Ca-X, and ΔH^0= -15.0 kJ mol^{-1} for hydrogen on (Ca,Na)-Y. The corresponding entropy change, ΔS^0, resulted to be -118 and -127 J mol^{-1} K^{-1}, respectively. Estimated error limits are ±0.8 kJ mol^{-1} for ΔH^0 and ±10 J mol^{-1} K^{-1} for ΔS^0. It should be noted that for obtaining the plots shown in Fig. 3 A_M has to be known. An approximate value of this parameter was obtained, in each case, by recording IR spectra for increasing doses of hydrogen at 77 K and extrapolating the resulting Langmuir-type isotherm. This approximate value was then refined by plotting the left-hand side of Eq. (3) against reciprocal temperature for A_M values which were changed in small steps around the original value, and selecting (by linear regression) the best fit to the whole set of experimental data. The basis of this method was explained in detail elsewhere [34].

The volumetric hydrogen adsorption isotherms obtained at 77.3 K on both zeolites, Ca-X and (Ca,Na)-Y are shown in Fig. 4; while Fig. 5 depicts the corresponding adsorption isotherms at 90.2 K. In every case, these hydrogen adsorption isotherms show two distinct regions; a very steep (nearly vertical) region at a very low pressure, followed by a second region where adsorbed volume becomes more dependent on equilibrium pressure. This experimentally observed behaviour suggests that two different adsorption processes occur in each case; such distinct processes will be analysed in some detail below. Let us first point out that the very steep initial region of the adsorption isotherms precludes precise determination of the isosteric heat of adsorption, q_{iso}, for the initial amounts of adsorbed hydrogen; in fact, unreasonable results were obtained when trying to calculate q_{iso} values corresponding to hydrogen adsorbed amounts smaller that about 10 cm^3 g^{-1} (STP). Disregarding this region, Fig. 6 shows the evolution of adsorption heat (q_{iso}) against adsorbed volume for hydrogen on Ca-X and on (Ca,Na)-Y; as determined from the corresponding adsorption isotherms at 77.3 and 90.2 K.

For hydrogen adsorbed on Ca-X, Fig. 6 shows an initial plateau, up to *ca*. 37 cm^3 g^{-1} (STP), where q_{iso} has a constant value of 12 kJ mol^{-1}; which coincides, within experimental error, with the value of ΔH^0 = -12.5(±0.8) kJ mol^{-1} determined by the spectroscopic VTIR method (as stated above). In the case of (Ca,Na)-Y, no precise initial value of q_{iso} could be obtained, because the corresponding plateau was not reached within the usable data range. However, extrapolation of the curve shown in Fig. 6 suggests that for the smallest hydrogen doses q_{iso} should be significantly greater than 12 kJ mol^{-1}, in agreement with the fact that a value of ΔH^0 = -15.0(±0.8) kJ mol^{-1} was determined by VTIR spectroscopy. Note that infrared spectroscopy monitors only H_2 molecules which are in direct (close) interaction with adsorbing cationic centres of the zeolite, and hence, the determined values of ΔH^0 correspond to the adsorption regime up to saturation of all Ca^{2+} cations with adsorbed H_2 molecules.

In both cases, H_2/Ca-X and H_2/(Ca,Na)-Y, the plot of q_{iso} against adsorbed hydrogen volume (Fig. 6) confirms that two different adsorption processes occur. First, adsorbed hydrogen molecules can come into direct contact with the zeolite Ca^{2+} cations, giving rise to localized adsorption involving the initial values of q_{iso} discussed above. For Ca-X, this process extends up to about 37 cm^3 g^{-1} (STP) of adsorbed hydrogen, while for (Ca,Na)-Y it only reaches up to about 12 cm^3 g^{-1}. This is in consonance with the expected smaller amount of Ca^{2+} ions per gram of zeolite in (Ca,Na)-Y, as compared with Ca-X; because of a higher Si:Al ratio in (Ca,Na)-Y, and also because of incomplete exchange of calcium for sodium. Once the cationic hydrogen adsorbing centres are all saturated, q_{iso} drops to a value of 4 to 6 kJ mol^{-1}; which is typical of unspecific (delocalized) adsorption processes involving only weak (London-type) interaction forces. Note that both, porous carbons and organic (porous) polymers, were repeatedly reported [1,37] to show a hydrogen adsorption heat in the range of 3.5 to 6.5 kJ mol^{-1}. A further comment concerns the observed fact (Fig. 6) that, after the initial adsorption process, q_{iso} falls down somewhat less steeply for the H_2/(Ca,Na)-Y system than for H_2/Ca-X. This observed difference is likely to be due, at least in part, to the presence (in the first case) of some Na^+ ions which, having a smaller polarizing power, are expected to contribute to hydrogen adsorption once all Ca^{2+} ions are saturated.

Additional information, particularly in regard to the weak interaction between hydrogen and the Ca-X zeolite, can be obtained from analysis of the hydrogen adsorption isotherms. Since the q_{iso} plot (Fig. 6) is composed of two regions, each of

them at a nearly constant q_{iso} value, it should be possible to adjust the adsorption data by using a sum of two Langmuir type isotherms, that can be written as:

$$N = [N_1 K_1/(1+pK_1)] + [N_2 K_2/(1+pK_2)] \quad (4)$$

where N is the total amount of adsorbed hydrogen, N_1 and N_2 the adsorbed amount corresponding to each of the adsorption regimes and K_1 and K_2 the equilibrium constant of the corresponding Langmuir equation. Note that each of the two terms in the right-hand side of eqn. (4) has a rather different meaning. The first term corresponds to the relatively strong interaction that involves localized adsorption on cation sites; the second term is the analytical representation of non-localized adsorption in micropores, which also follows a Langmuir-type equation, as shown by Bathia and Myers for carbons [37]. Eq. (4) was used to fit the data of the adsorption isotherm (at 77.3 K) of hydrogen on Ca-X, depicted in Fig. 4. The result, shown in Fig. 7, confirms that a satisfactory fit could indeed be obtained. The fitting parameters corresponding to the strong interaction resulted to be N_1= 37.5(±0.5) $cm^3\ g^{-1}$ (STP) and K_1= 79(±2) $Torr^{-1}$. The correctness of these values can readily be checked; the former coincides with the sudden change in q_{iso} (Fig. 6), while the latter corresponds to a ΔG^0 value of -2.80 kJ mol^{-1} as obtained from the standard Gibbs equation, $\Delta G^0 = -RT\ln K_1$. Since the corresponding ΔH^0 value is -12.5 kJ mol^{-1}, ΔS^0 results to be -126 J $mol^{-1}\ K^{-1}$; a value which coincides (within experimental error) with that of ΔS^0= -118(±10) J $mol^{-1}\ K^{-1}$ obtained independently by variable-temperature IR spectroscopy. For the second term of the sum in Eq. (4), which accounts for the weak interaction, the corresponding fitting parameters resulted to be, N_2= 159(±1.5) $cm^3\ g^{-1}$ (STP) and K_2= 2.15(±0.05)×10^{-3} $Torr^{-1}$. This value of K_2 yields ΔG^0 = -3.93 kJ mol^{-1}, and since q_{iso} (which differs from ΔH^0 by a mere RT term) has a value of about 5 kJ mol^{-1} (Fig. 6), the corresponding entropy change results to be of about - 122 J $mol^{-1}\ K^{-1}$. A similar calculation would not go well for the H_2/(Ca,Na)-Y system, because (for the reasons already commented upon) the curve describing the experimentally determined variation of q_{iso} as a function of hydrogen adsorbed amount cannot be neatly divided into two parts, each of them showing a (nearly) constant q_{iso} value. Hence, modelling of the adsorption isotherm would imply putting at least three summing terms on the right-hand side of Eq. (4);

which would lead to having too many adjustable parameters, and to corresponding uncertainty arising from correlation effects.

Finally, it seems pertinent to analyse the results here reported for the standard adsorption enthalpy and entropy of molecular hydrogen on calcium-exchanged faujasites in the context of corresponding data for other alkaline zeolites. For that purpose, Table 1 summarizes recently reported data [38-40] of ΔH^0 and ΔS^0 for hydrogen adsorption on several alkali and alkaline-earth cation exchanged zeolites, together with those here reported for Ca-X and (Ca,Na)-Y. Note that these ΔH^0 and ΔS^0 values correspond to the process involving (cation) localized hydrogen adsorption, which is the only one measured by the VTIR method. These data clearly show, as discussed in detail elsewhere [39], that there is a non-linear correlation between hydrogen adsorption enthalpy and entropy, in the sense that (in general terms) larger values of ΔH^0 involve larger values of ΔS^0. Such a correlation can best be appreciated in Fig. 8, where ΔH^0 is plotted against ΔS^0. Clearly, the points corresponding to (Ca,Na)-Y and to Ca-X fit well into the correlation curve, thus given further confidence on the results here reported.

Enthalpy-entropy correlation (also termed compensation) was also reported to occur in a wide range of chemical processes involving relatively weak interaction forces [41-43]. For the case of hydrogen adsorption on zeolites such a correlation reflects the fact that a stronger (enthalpy related) interaction between hydrogen molecules and zeolite adsorbing centres leads to a larger decrease of motion freedom of the adsorbed molecules, and hence to (entropy related) greater order of the system. It should also be noted that there is an intrinsic limit for ΔS^0, since each adsorbed molecule can lose no more than all of its degrees of motion freedom, while in principle no definite limit exists for ΔH^0; and this would explain the increasing slope of the curve representing the plot of ΔH^0 against ΔS^0 (Fig. 8) when ΔS^0 increases more and more. ΔS^0 data reported in Fig. 8 were obtained by VTIR spectroscopy, and they are referred to a standard state at 1 Torr (1.32 mbar) and 100 K, representative of the pressure and temperature range at which IR spectra were obtained. Since the entropy content of 1 mol of hydrogen at 1 Torr and 100 K is of about 175 kJ mol^{-1}, this would be the uppermost limit of ΔS^0. However, this limit is not likely to be attained, because adsorbed hydrogen molecules are known to preserve a certain degree of rotational freedom, as well as vibration

against the zeolite adsorbing centre [18,31,44]. Whichever the case, however, we wish to remark that the observed correlation between enthalpy and entropy changes upon adsorption should be taken into account when designing potential adsorbents for storage and delivery of molecular hydrogen.

Conclusions

Thermodynamics of hydrogen adsorption on the zeolites Ca-X and (Ca,Na)-Y was studied by combining variable-temperature IR (VTIR) spectroscopy with volumetric measurements of hydrogen adsorption at 77.3 and 90.2 K. The case of Ca-X, the simplest of the two here examined, clearly shows that two types of interaction mode are possible for hydrogen molecules on cationic zeolites. The first of these modes involves a relatively strong electrostatic interaction of the adsorbed H_2 molecules with the exposed metal cation centres; such an interaction results in polarization of the adsorbed molecule, which renders the H–H stretching mode IR active. Moreover, for Ca-X, the interaction sites appear to be all of them equivalent and non mutually interacting, thus giving rise to a plateau in the initial portion of the plot of isosteric heat of adsorption against surface coverage. This indicates an ideal, Langmuir-type, nature of adsorption which is confirmed by the applicability of the VTIR spectroscopic method.

Further to that, a non specific (delocalized) adsorption mode takes place presumably once all of the exposed metal cations are saturated. This second adsorption mode, which corresponds to the filling of zeolite pores, shows a smaller interaction energy, similar to that reported for hydrogen adsorption on porous carbons and which can be assigned to weak (dispersion-type) interaction forces. It is remarkable that this second adsorption process can also be described by a Langmuir-type adsorption isotherm.

For the case of (Ca,Na)-Y, the results are somewhat blurred because of incomplete cation exchange. However, in general terms, the basic concepts stated above can still be applied. VTIR spectroscopy still shows an initially strong interaction due to localized adsorption of hydrogen molecules on Ca^{2+} cation centres, followed by a weaker interaction mode which should correspond to the ensuing pore filling at higher H_2 equilibrium pressure.

The standard adsorption enthalpy, ΔH^0, for the strong interaction mode was found to be -12.5 and -15.0 kJ mol^{-1} for Ca-X and (Ca,Na)-Y, respectively. Such a relatively large values of ΔH^0 were found to involve also correspondingly large values

of adsorption entropy: -118 and -127 J mol^{-1} K^{-1} for hydrogen adsorption on Ca-X and Ca-Y, respectively, referred to an standard state at 1 Torr and 100 K. Indeed, both systems, H_2/Ca-X and H_2/(Ca,Na)-Y, conform to an overall enthalpy-entropy compensation effect already observed for hydrogen adsorption on other alkali and alkaline-earth cation exchanged zeolites.

Acknowledgements

Financial support from Regione Piemonte (CIPE Project C72), MUR (2004 FISR Project "Vettore Idrogeno"), Spanish MEC and FEDER funds (Project MAT2005-05350) and from the Conselleria d'Economia, Hisenda e Innovació de les Illes Balears (Project PROGECIB-22A) is gratefully acknowledged.

References

[1] Van den Berg AWC, Areán CO. Materials for hydrogen storage: current research trends and perspectives. Chem Commun 2008:668-681.
[2] Thomas KM. Hydrogen adsorption and storage on porous materials. Catal Today 2007;120:389-398.
[3] Ansón A, Jagiello J, Parra JB, Sanjuán ML, Benito AM, Maser WK, Martínez MT. Porosity, surface area, surface energy, and hydrogen adsorption in nanostructured carbons. J Phys Chem B 2004;108:15820-15826.
[4] Ströbel R, Garche J, Moseley PT, Jörissen L, Wolf G. Hydrogen storage by carbon materials. J Power Sources 2006;159:781-801.
[5] Jordá-Beneyto M, Lozano-Castelló D, Suárez-García F, Cazorla-Amorós D, Linares-Solano A. Advanced activated carbon monoliths and activated carbons for hydrogen storage. Microporous Mesoporous Mater 2008;112:235-242.
[6] Yang Z, Xia Y, Mokaya R. Enhanced hydrogen storage capacity of high surface area zeolite-like carbon materials. J Am Chem Soc 2007;129:1673-1679.
[7] Kowalczyk P, Holyst R, Terrones M, Terrones H. Hydrogen storage in nanoporous carbon materials: myth and facts. Phys Chem Chem Phys 2007;15:1786-1792.
[8] Armandi M, Bonelli B, Arean CO, Garrone E. Role of microporosity in hydrogen adsorption on templated nanoporous carbons. Microporous Mesoporous Mater 2008;112:411-418.
[9] Rosi NL, Eckert J, Eddaoudi M, Vodak T, Kim J, O'Keeffe M, Yaghi OM. Hydrogen storage in microporous metal-organic frameworks. Science 2003;300:1127-1129.
[10] Zhao X, Xiao B, Fletcher AJ, Thomas KM, Bradshaw D, Rosseinsky MJ. Hysteretic adsorption and desorption by nanoporous metal-organic frameworks. Science 2004;306:1012-1015.
[11] Roswell JLC, Yaghi OM. Strategies for hydrogen storage in metal-organic frameworks. Angew Chem Int Ed 2005;44:4670-4679.
[12] Yang Q, Zhong C. Understanding hydrogen adsorption in metal-organic frameworks with open metal sites: a computational study. J Phys Chem B 2006;110:655-658.

[13] Collins DJ, Zhou HC. Hydrogen storage in metal-organic frameworks. J Mater Chem 2007;30:3154-3160.
[14] Mulder FM, Dingemans TJ, Schimmel HG, Ramirez-Cuesta AJ, Kearley GJ. Hydrogen adsorption strength and sites in the metal organic framework MOF5: Comparing experiment and model calculations. Chem Phys 2008;351:72-76.
[15] Kaye SS, Long JR. Hydrogen adsorption in dehydrated variants of the cyano-bridged framework compunds $A_2Zn_3[Fe(CN)_6]_2 \cdot xH_2O$ (A= H, Li, Na, K, Rb). Chem Commun 2007:4486-4488.
[16] Regli L, Zecchina A, Vitillo JG, Cocina D, Spoto G, Lamberti C, Lillerud KP, Olsby U, Bordiga S. Hydrogen storage in chabazite zeolite frameworks. Phys Chem Chem Phys 2005;7:3197-3203.
[17] Dong J, Wang X, Xu H, Zhao Q, Li J. Hydrogen storage in several microporous zeolites. Int J Hydrogen Energy 2007;32:4998-5004.
[18] Ramirez-Cuesta AJ, Mitchell PCH, Ross DK, Georgiev PA, Anderson PA, Langmi HW, Book D. Dihydrogen in cation-substituted zeolites X: an inelastic neutron scattering study. J Mater Chem 2007;17:2533-2539.
[19] Areán CO, Manoilova OV, Bonelli B, Delgado MR, Palomino GT, Garrone E. Thermodynamics of hydrogen adsorption on the zeolite Li-ZSM-5. Chem Phys Lett 2003;370:631-635.
[20] Prasanth KP, Pillai RS, Bajaj HC, Jasra RV, Chung HD, Kim TH, Song SD. Adsorption of hydrogen in nickel and rhodium exchanged zeolites X. Int J Hydrogen Energy 2008;33:735-745.
[21] Areán CO, Nachtigallova D, Nachtigall P, Garrone E, Delgado MR. Thermodynamics of reversible gas adsorption on alkali-metal exchanged zeolites: the interplay of infrared spectroscopy and theoretical calculations. Phys Chem Chem Phys 2007;9:1421-1437.
[22] Torres FJ, Civalleri B, Pisani C, Ugliengo P. An ab initio study of acidic chabazite as a candidate for dihydrogen storage. J Phys Chem B 2006;110:10467-10474.
[23] Nachtigall P, Garrone E, Palomino GT, Delgado MR, Nachtigallova D, Areán CO. FTIR spectroscopic and computational studies on hydrogen adsorption on the zeolite Li-FER. Phys Chem Chem Phys 2006;8:2286-2292.
[24] Torres FJ, Vitillo JG, Civalleri B, Ricchiardi G, Zecchina A. Interaction of H_2 with alkali-metal-exchanged zeolites: a quantum mechanical study. J Phys Chem C 2007;111:2505-2513.
[25] Kang L, Deng W, Han K, Zhao T, Liu Z. A DFT study of adsorption hydrogen on the Li-FAU zeolite. Int J Hydrogen Energy 2008;33:105-110.
[26] Torres FJ, Ugliengo P, Civalleri B, Terentyev A, Pisani C. A review of the computational studies of proton and metal-exchanged chabazites as media for molecular hydrogen storage performed with the CRYSTAL code. Int J Hydrogen Energy 2008;33:746-754.
[27] Szostak RM. Molecular sieves: Principles of synthesis and identification. Van Nostrand Reinhold, New York, 1989.
[28] Treacy MMJ, Higgins JB. Collection of simulated XRD powder patterns for zeolites. Elsevier, 2001.
[29] Tsyganenko AA, Storozhev PY, Arean CO. Infrared spectroscopic studies on the binding isomerism of adsorbed molecules. Kinet Catal 2004;45:530-540.
[30] Kazansky VB, Borovkov VY, Karge HG. Diffuse reflectance IR study of molecular hydrogen and deuterium adsorbed at 77 K on NaA zeolite .1. Fundamentals, combination and vibrational-rotational modes. J Chem Soc Faraday Trans 1997;93:1843-1848.

[31] Kazansky VB. DRIFT spectra of adsorbed dihydrogen as a molecular probe for alkaline metal ions in faujasites. J Mol Catal A 1999;141:83-94.
[32] Palomino GT, Carayol MRL, Areán CO. Hydrogen adsorption on magnesium-exchanged zeolites. J Mater Chem 2006;16:2884-2885.
[33] Areán CO, Manoilova OV, Palomino GT, Delgado MR, Tsyganenko AA, Bonelli, B, Garrone E. Variable-temperature infrared spectroscopy: An access to adsorption thermodynamics of weakly interacting systems. Phys Chem Chem Phys 2002;4:5713-5715.
[34] Garrone E, Areán CO. Variable temperature infrared spectroscopy: A convenient tool for studying the thermodynamics of weak solid-gas interactions. Chem Soc Rev 2005;34:846-857.
[35] Vitillo JG, Damin A, Zecchina A, Ricchiardi G. Theoretical characterization of dihydrogen adducts with alkaline cations. J Chem Phys 2005;122:article number 114311.
[36] Bordiga S, Garrone E, Lamberti C, Zecchina A, Areán CO, Kazansky VB, Kustov LM. Comparative IR spectroscopic study of low temperature H_2 and CO adsorption on Na-zeolites. J Chem Soc Faraday Trans 1994;90:3367-3372.
[37] Bhatia SK, Myers AL. Optimum conditions for adsorptive storage. Langmuir 2006;22:1688-1700.
[38] Areán CO, Palomino GT, Carayol MRL. Variable temperature FT-IR studies on hydrogen adsorption on the zeolite (Mg,Na)-Y. Appl Surf Sci 2007;253:5701-5704.
[39] Garrone E, Bonelli B, Areán CO. Enthalpy-entropy correlation for hydrogen adsorption on zeolites. Chem Phys Lett 2008;456:68-70.
[40] Areán CO, Palomino GT, Garrone E, Nachtigallova D, Nachtigall P. Combined theoretical and FTIR spectroscopic studies on hydrogen adsorption on the zeolites Na-FER and K-FER. J Phys Chem B 2006;110:395-402.
[41] Dunitz JD. Win some, lose some: enthalpy-entropy compensation in weak intermolecular interactions. Chem Biol 1995;2:709-712.
[42] Westwell MS, Searle MS, Klein J, Williams DH. Successful predictions of the residual motion of weakly associated species as a function of the bonding between them. J Phys Chem 1996;100:16000-16001.
[43] Liu L, Guo QX. Isokinetic relationship, isoequilibrium relationship, and enthalpy-entropy compensation. Chem Rev 2001;101:673-695.
[44] Ramírez-Cuesta AJ, Mitchell PCH, Ross DK, Georgiev PA, Anderson PA, Langmi HW, Book D. Dihydrogen in zeolite CaX: an inelastic neutron scattering study. J Alloys Compd 2007;446-447:393-396.

Table 1. Spectroscopic and thermodynamic data for hydrogen adsorbed on several zeolites. Error limits for ΔH^0 and ΔS^0 are ±1 kJ mol^{-1} and ±10 J mol^{-1} K^{-1}, respectively.

Zeolite	ν(H–H) (cm^{-1})	$-\Delta H^0$ (kJ mol^{-1})	$-\Delta S^0$ (J mol^{-1} K^{-1})	Ref.
(Mg,Na)-Y	4056	18	136	38
(Ca,Na)-Y	4078	15	127	This work
Ca-X	4082	12.5	116	This work
Mg-X	4066	11	103	39
Na-FER	4100	6	78	40
Li-ZSM-5	4092	6.5	90	19
Na-ZSM-5	4101	10.3	121	21,39

Figure captions

Figure 1. Variable Temperature FT-IR spectra (zeolite blank subtracted) in the H–H stretching region, of H_2 adsorbed on Ca-X. Temperature, in K, and equilibrium pressure (Torr, in brackets) are shown (1 Torr = 1.32 mbar).

Figure 2. Variable Temperature FT-IR spectra (zeolite blank subtracted) in the H–H stretching region, of H_2 adsorbed on (Ca,Na)-Y. Temperature, in K, and equilibrium pressure (Torr, in brackets) are shown (1 Torr = 1.32 mbar).

Figure 3a. Plot of the left-hand side of Equation (3) against reciprocal temperature for H_2/Ca-X. R, linear regression coefficient; SD, standard deviation.

Figure 3b. As in 3a: H_2/(Ca,Na)-Y system.

Figure 4. Volumetric hydrogen adsorption isotherms at 77.3 K on Ca-X (squares) and on (Ca,Na)-Y (circles) zeolites. Black symbols denote adsorption and white ones desorption.

Figure 5. Volumetric hydrogen adsorption isotherms at 90.2 K on Ca-X (squares) and on (Ca,Na)-Y (circles) zeolites.

Figure 6. Evolution of adsorption heat (q_{iso}, kJ mol^{-1}) against adsorbed volume (cm^3 g^{-1}, STP) for hydrogen on Ca-X (squares) and on (Ca,Na)-Y (circles); as determined for the corresponding adsorption isotherms at 77.3 and 90.2 K.

Figure 7. Volumetric hydrogen adsorption isotherm at **77.3** K on Ca-X zeolite (squares), with the corresponding fitting curve obtained according to Equation (4).

Figure 8. Standard adsorption enthalpy versus entropy for hydrogen adsorption on several cation exchanged zeolites. The two stars refer to values obtained in this work with Ca-X and (Ca,Na)-Y.

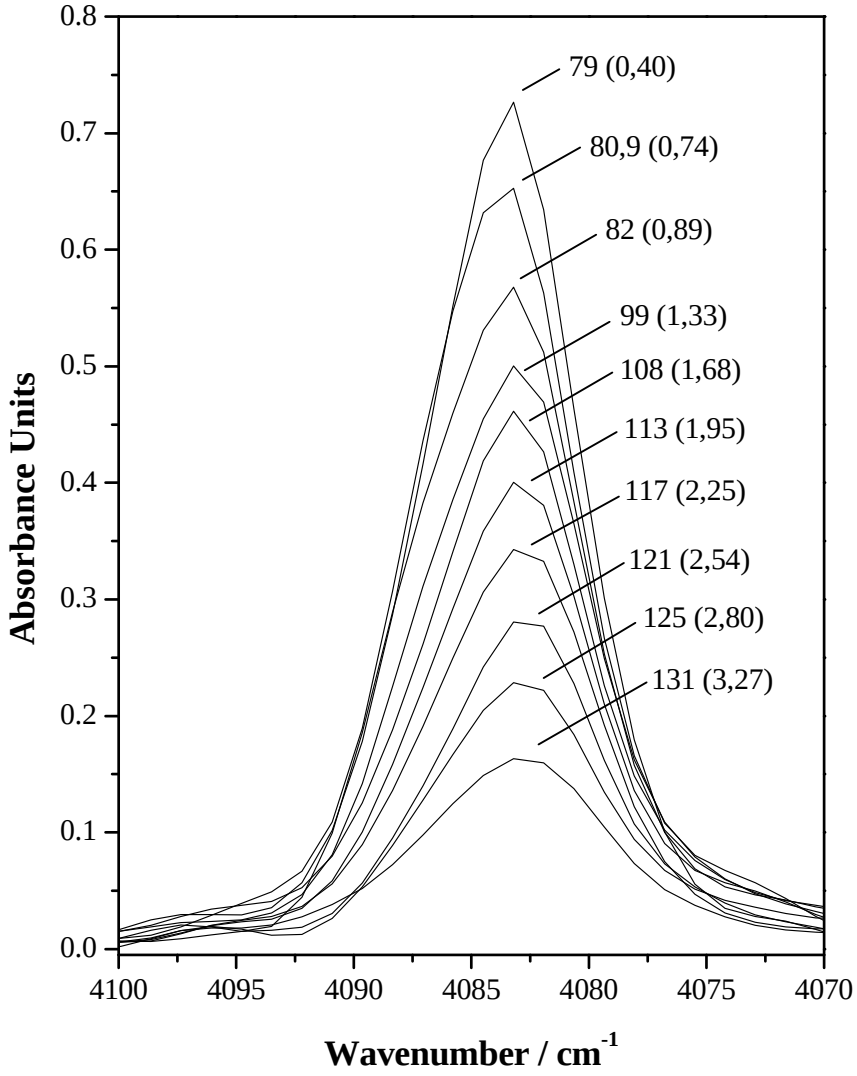
0.8
0.7
0.6
0.5
0.4
0.3
0.2
0.1
0.0
Absorbance Units
4100
4095
4090
4085
4080
4075
4070
Wavenumber / cm-1
79 (0,40)
80,9 (0,74)
82 (0,89)
99 (1,33)
108 (1,68)
113 (1,95)
117 (2,25)
121 (2,54)
125 (2,80)
131 (3,27)

Figure 1

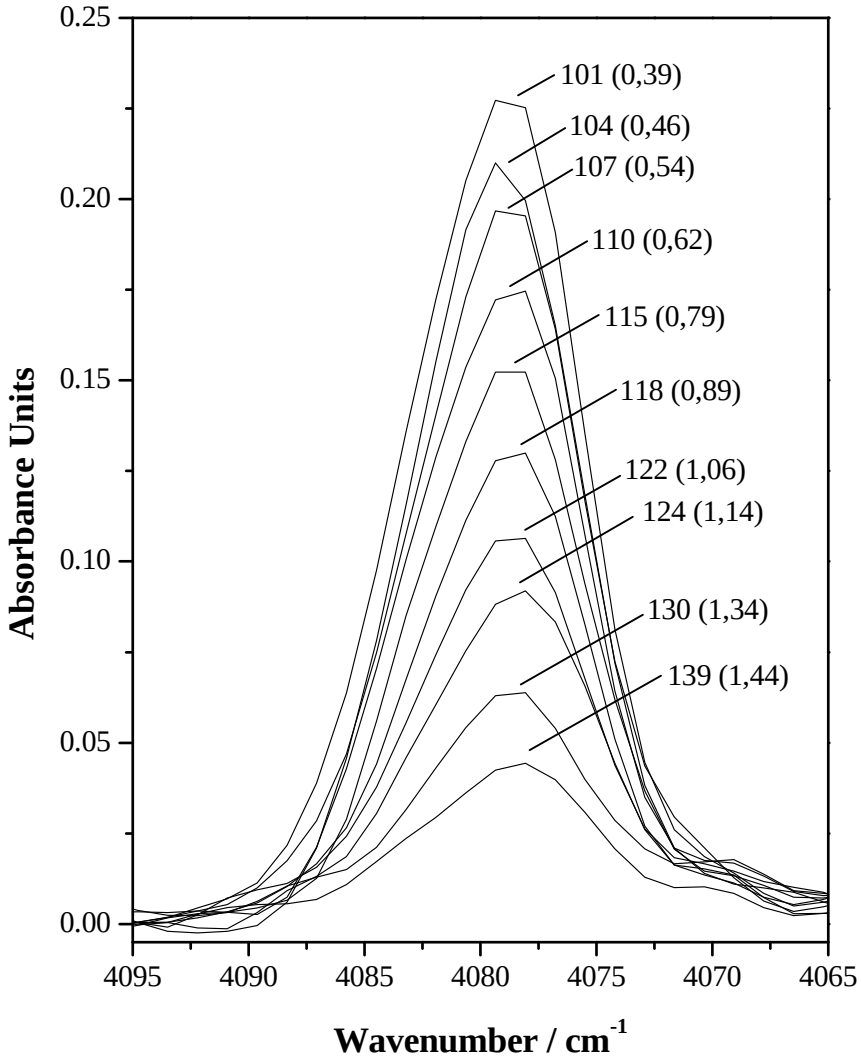
0.25
0.20
0.15
0.10
0.05
0.00
Absorbance Units
101 (0,39)
104 (0,46)
107 (0,54)
110 (0,62)
115 (0,79)
118 (0,89)
122 (1,06)
124 (1,14)
130 (1,34)
139 (1,44)
4095
4090
4085
4080
4075
4070
4065
Wavenumber / cm-1

Figure 2

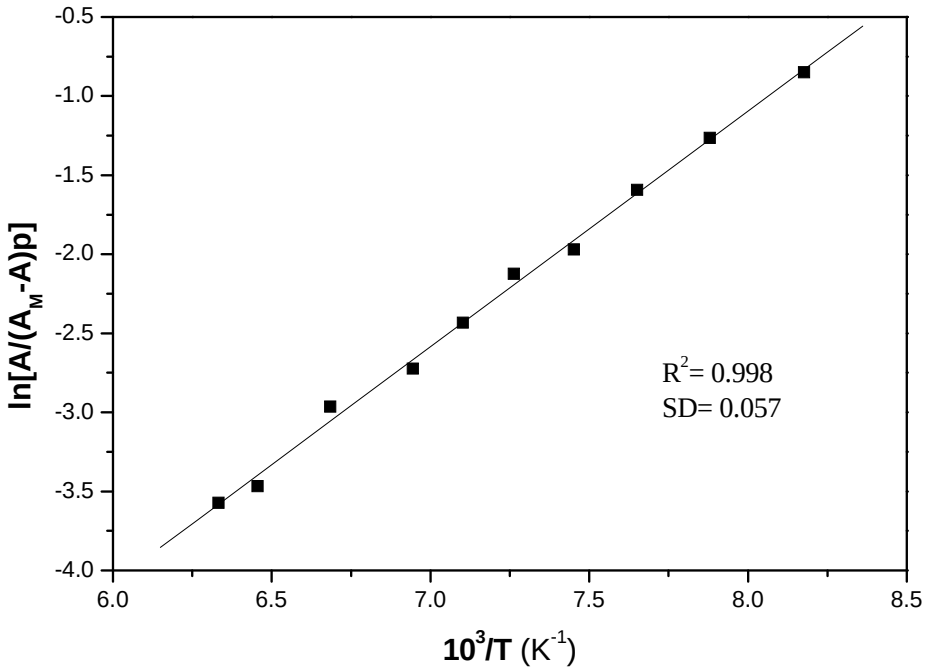

Figure 3a

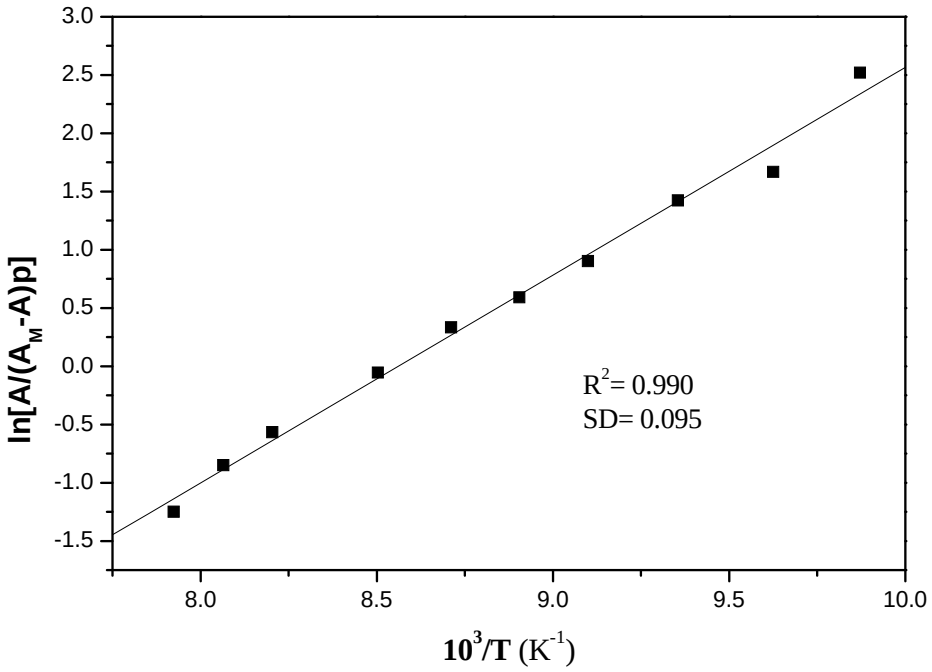

Figure 3b

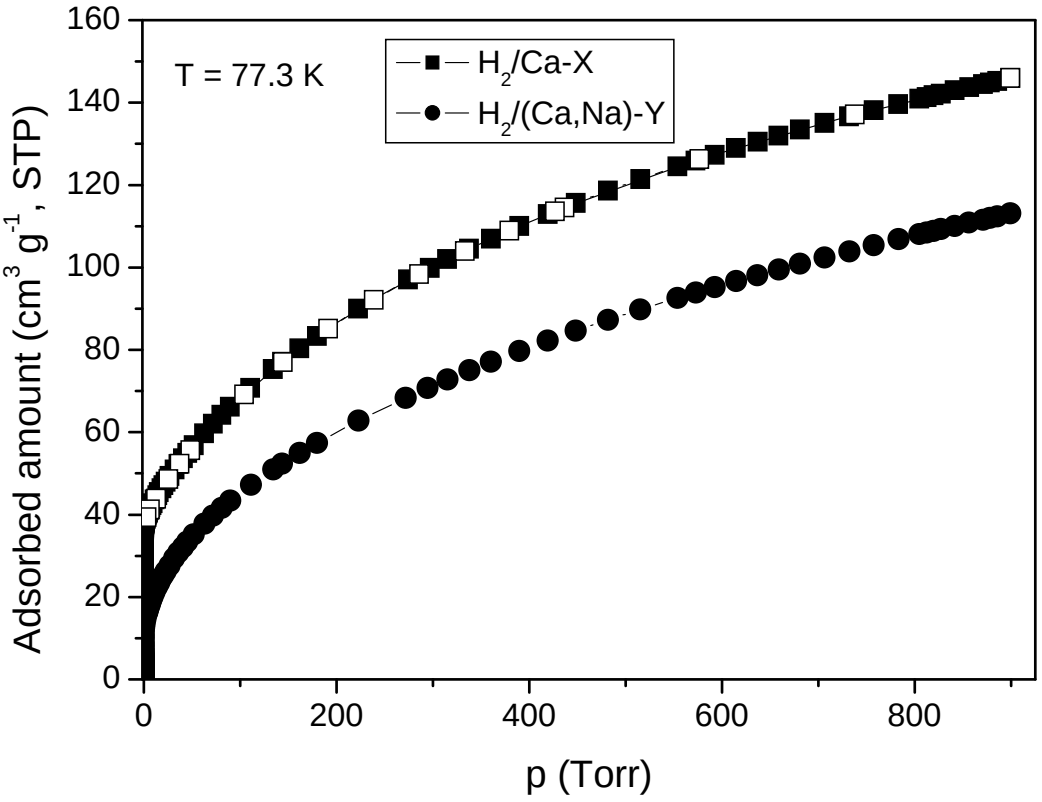
T = 77.3 K
H2/Ca-X
H2/(Ca,Na)-Y
Adsorbed amount (cm3 g-1, STP)
p (Torr)
0
20
40
60
80
100
120
140
160
0
200
400
600
800

Figure 4

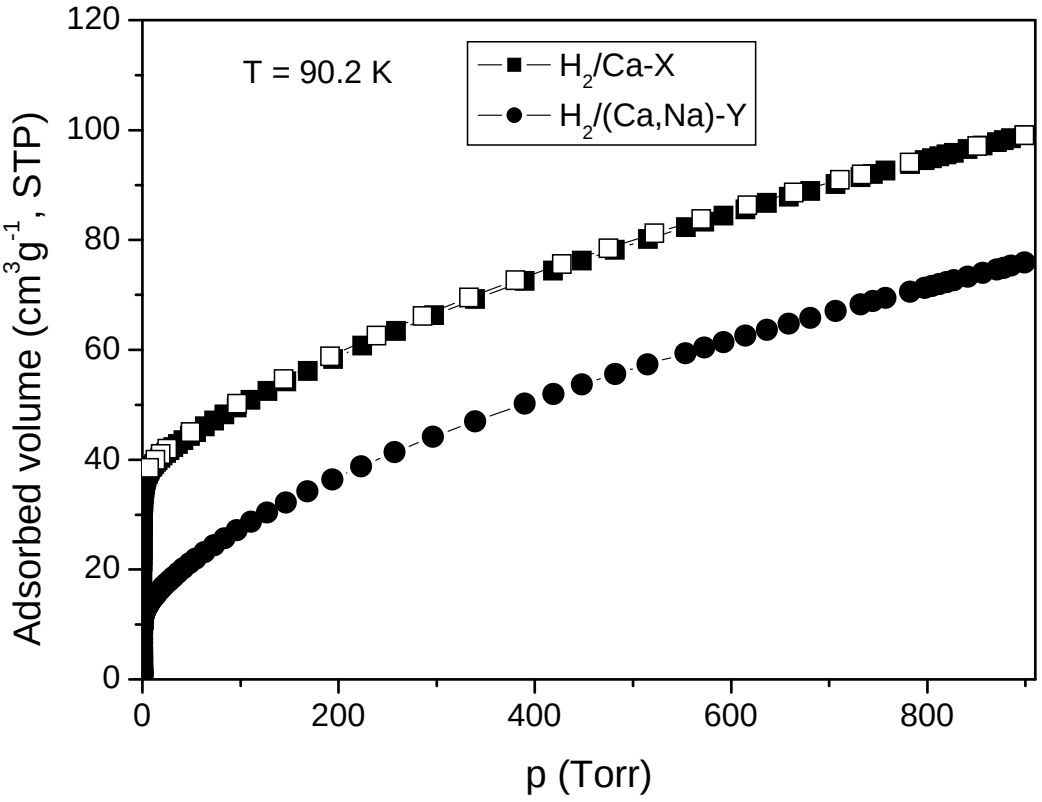
T = 90.2 K
H2/Ca-X
H2/(Ca,Na)-Y
Adsorbed volume (cm3g-1, STP)
p (Torr)
0
20
40
60
80
100
120
0
200
400
600
800

Figure 5

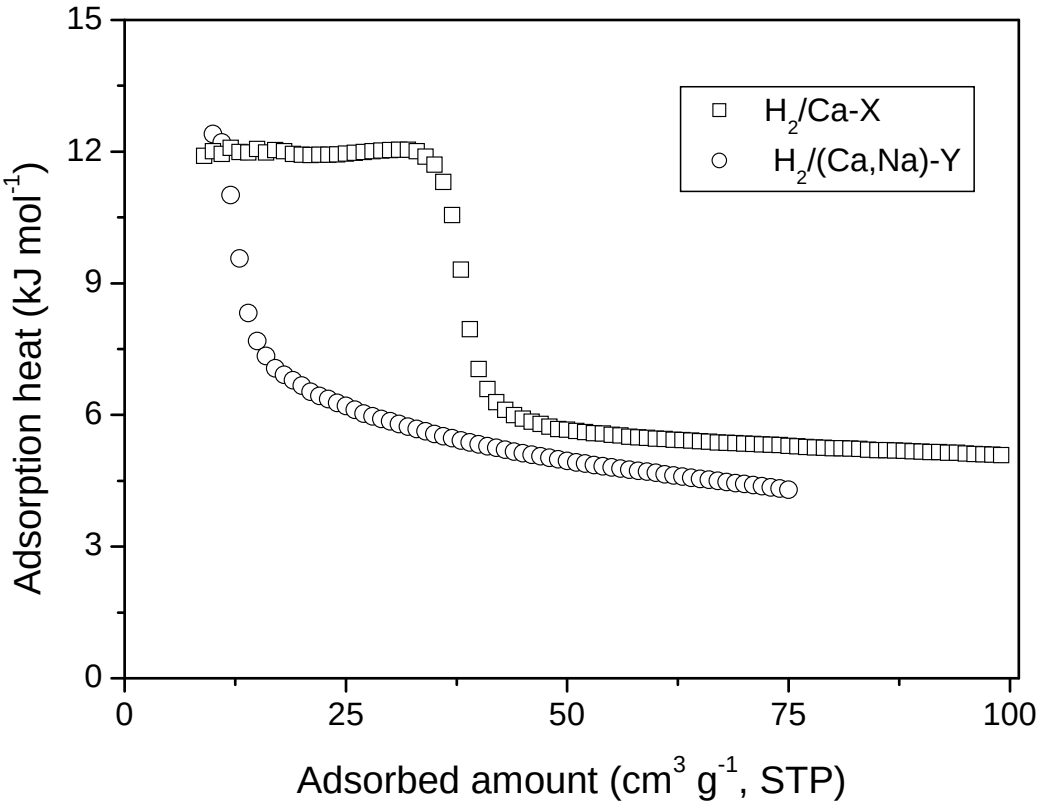
15
12
9
6
3
0
0
25
50
75
100
Adsorption heat (kJ mol-1)
Adsorbed amount (cm3 g-1, STP)
H2/Ca-X
H2/(Ca,Na)-Y

Figure 6

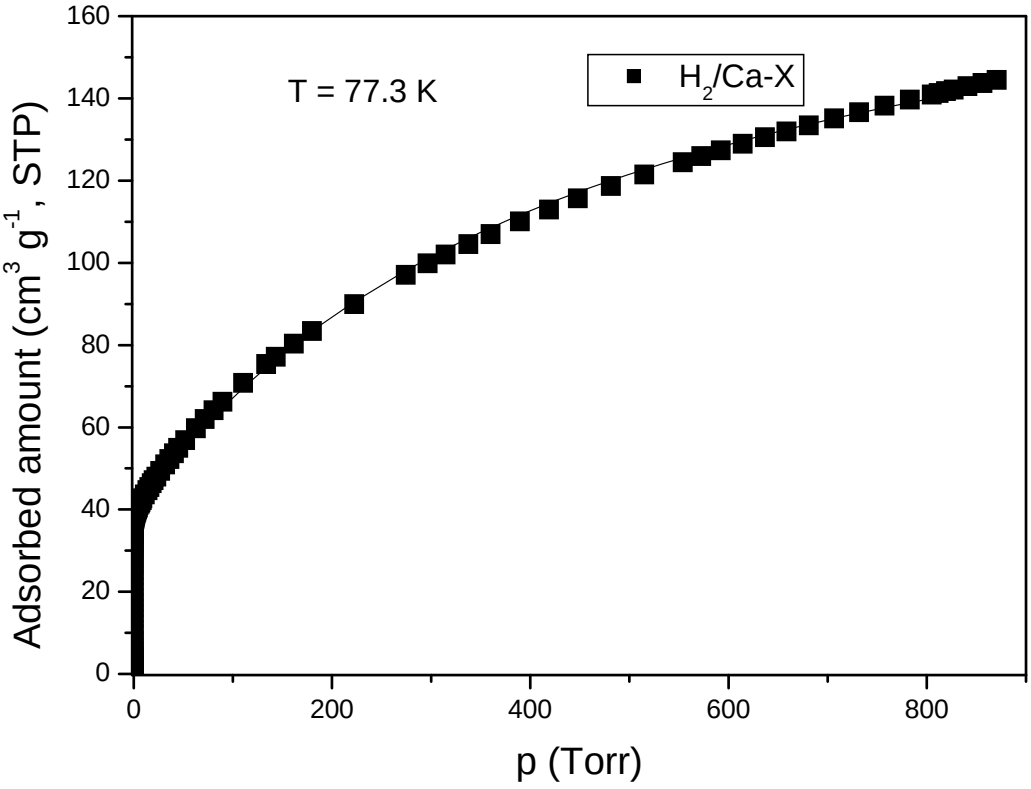
T = 77.3 K
H2/Ca-X
Adsorbed amount (cm3 g-1, STP)
p (Torr)
0
20
40
60
80
100
120
140
160
0
200
400
600
800

Figure 7

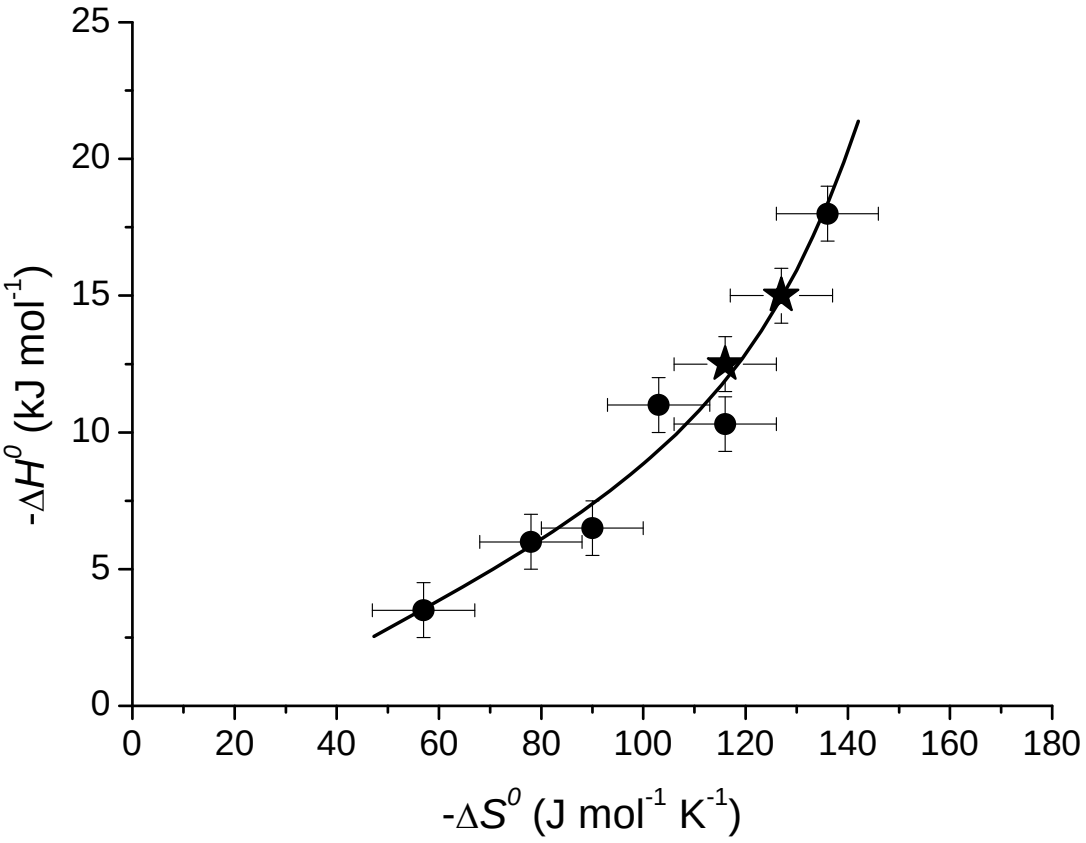
25
20
15
10
5
0
0
20
40
60
80
100
120
140
160
180
-ΔH⁰ (kJ mol⁻¹)
-ΔS⁰ (J mol⁻¹ K⁻¹)

Figure 8